# On Modeling Multi-Antenna Multipath Channels

**Article** · November 2000

Source: CiteSeer



**1 author:**

Akbar M Sayeed
University of Wisconsin–Madison
**271** PUBLICATIONS **8,029** CITATIONS

# On Modeling Multi-Antenna Multipath Channels

Akbar M. Sayeed*

Department of Electrical and Computer Engineering
University of Wisconsin–Madison
1415 Engineering Drive
Madison, WI 53706
akbar@engr.wisc.edu, http://dune.ece.wisc.edu

38th Annual Allerton Conference, October 2000.

**Abstract**

Accurate and tractable channel modeling is critical to realizing the full potential of antenna arrays in wireless communications. In this paper we propose a framework for modeling multi-antenna multipath channels based on the notion of virtual spatial angles. The virtual angles are fixed a priori and are determined by the number of antennas at the transmitter and receiver and the spacing between the antennas. The model essentially corresponds to a coordinate transformation via fixed spatial basis functions (array response and steering vectors) at the transmitter and receiver. The resulting linear channel matrix representation in the virtual space encompasses all existing models and provides a natural link between the actual physical propagation environment and the channel statistics induced by it. For any given scattering environment, the model clearly reveals the two key parameters affecting channel capacity: the number of parallel channels and the level of diversity associated with each parallel channel. In addition to facilitating realistic estimates of channel capacity, the virtual space framework also suggests low-complexity channel approximations that may be leveraged in efficient transceiver design.

## 1 Introduction

The use of antenna arrays holds great promise for bandwidth-efficient communication over the harsh wireless channel. The advantages of antenna arrays are many-fold. They provide additional diversity to combat fading that can be exploited via appropriate space-time signaling and coding to enhance system capacity. They can be used for spatially selective signaling and reception to mitigate multiuser interference. Finally, antenna arrays also provide additional dimensions/degrees of freedom that can be exploited for efficient allocation of network resources, such as power and bandwidth, to accommodate disparate requirements of different users. All these attractive features have motivated a great deal of research into the use of antenna arrays in mobile wireless communications.

Maximal exploitation of antenna arrays in wireless communication necessitates accurate yet computationally tractable modeling of the multi-input multi-output (MIMO) channel coupling the transmitters and receivers. Existing models represent two extreme approaches. On the one hand are *statistical* models that are idealized abstractions

*This research was supported in part by the National Science Foundation under CAREER grant CCR-9875805 and grant ECS-9979408, and by the Wisconsin Alumni Research Foundation.

of spatial propagation characteristics and assume independent fading between different transmit-receive element pairs. These models have been heavily used in capacity calculations and development of space-time coding techniques (see, e.g., [1, 2, 3]). On the other hand are *physical* models, inspired by array processing techniques, that explicitly model signal copies arriving from different directions. While more accurate descriptions of the actual propagation environment, these models are nonlinear in spatial angles, thereby making it rather difficult to incorporate them in transceiver design and capacity computations. Finally, the two approaches to MIMO antenna array modeling exist in virtual isolation without explicit connections relating them. A connection is very much desirable so that conclusions and insights derived from the two approaches can be combined and leveraged into improved transceiver designs.

There have been some recent attempts at bridging the gap between the two modeling philosophies (see, e.g., [4, 5]). However, these approaches are heavily entrenched in the physical modeling paradigm and suffer from the drawbacks associated with nonlinear modeling. We propose an approach, inspired by modeling physical propagation characteristics in the context of spatial signal space dimensions, that keeps the essence of physical modeling without its complexity and imposes a natural structure on channel statistics. Specifically, we model the channel with respect to fixed spatial basis functions defined by fixed virtual angles. This yields a linear channel characterization that is significantly more tractable analytically and also facilitates tackling various issues with ease. For instance, it explicitly reveals the level of spatial diversity afforded by the channel, a factor that critically affects outage capacity. In the context of spatio-temporal signal processing, the model provides a natural approach for spatially selective signaling at the transmitter and low-complexity processing at the receiver. Finally, despite its simplicity, the model encompasses *all* existing approaches to modeling spatial multipath channels.

The next section introduces the three signal spaces for describing a multi-antenna multipath channel: the element space (statistical model), the physical space, and the proposed virtual space. Section 3 discusses various aspects of the virtual space model, including relation to the other two models and statistical channel characterization. Section 4 illustrates the utility of the proposed channel model via outage capacity calculations in a variety of scenarios. Section 5 provides some concluding remarks about extensions.

# 2 Element, Physical, and Virtual Spaces

Consider a transmitter array with $n_T$ elements and a receiver array with $n_R$ elements. In the absence of noise, the transmitted and received signals are related as

$$\boldsymbol{x} = \boldsymbol{H}\boldsymbol{s} \tag{1}$$

where $\boldsymbol{s}$ is the $n_T$ dimensional transmitted signal, $\boldsymbol{x}$ is the $n_R$ dimensional received signal and $\boldsymbol{H}$ denotes the channel matrix coupling the transmitter and receiver elements. This is the *element space* (ES) description of the spatial channel. Most capacity calculations use this model and assume $\boldsymbol{H}$ to consist of independent, identically distributed (iid) Gaussian random variables — an idealized, rich scattering environment.

Explicit modeling of physical propagation effects can be used to impose structure on $\boldsymbol{H}$ as illustrated in Figure 1. The most widely used *physical space* (PS) model is

$$\boldsymbol{H} = \sum_{l=1}^{L} \beta_l \boldsymbol{a}_R(\phi_{R,l})\boldsymbol{a}_T^H(\phi_{T,l}) = \boldsymbol{A}_R(\underline{\phi}_R)\boldsymbol{H}_P\boldsymbol{A}_T^H(\underline{\phi}_T) \tag{2}$$

which couples the transmitter and the receiver via $L$ propagation paths with $\{\phi_{T,l}\}$ and $\{\phi_{R,l}\}$ as the spatial angles seen by the transmitter and receiver, respectively, and $\{\beta_l\}$ as the corresponding fading gains. In (2), $\boldsymbol{a}_R(\phi_R)$ represents the array response vector for a plane wave arriving from the direction $\phi_R$ and $\boldsymbol{a}_T(\phi_T)$ represents the transmitter steering

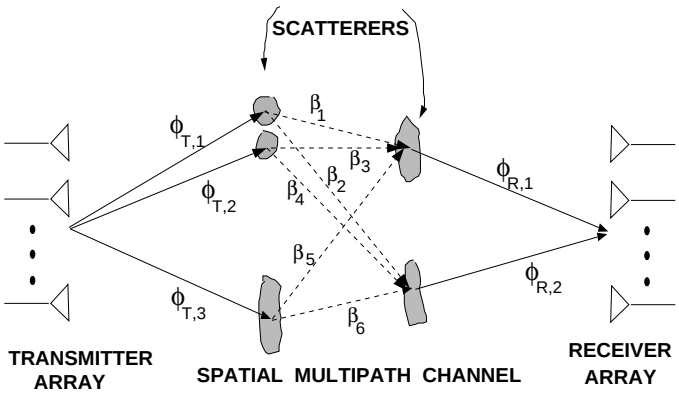


Figure 1: *A schematic illustrating channel modeling in the* **physical space**. *Each scattering path is associated with a fading gain ($\beta_l$) and a unique pair of transmit and receive angles ($\phi_{T,l}$, $\phi_{R,l}$) that connect physical scatterers arbitrarily distributed within the angular channel spreads.*

vector for the direction $\phi_T$. The angles $\{\phi_{R,l}\}$ lie in within $S_R$, the angular spread of scatterers as seen by the receiver, whereas $\{\phi_{T,l}\}$ lie within $S_T$, the angular spread of scatterers as seen by the transmitter. In the matrix representation in (2), $\boldsymbol{A}_R(\underline{\phi}_R) = [\boldsymbol{a}_R(\phi_{R,1}), \cdots, \boldsymbol{a}_R(\phi_{R,L})]$ is an $n_R \times L$ matrix, $\boldsymbol{A}_T(\underline{\phi}_T) = [\boldsymbol{a}_T(\phi_{T,1}), \cdots, \boldsymbol{a}_T(\phi_{T,L})]$ is an $n_T \times L$ matrix, and $\boldsymbol{H}_P = \mathrm{diag}(\beta_1, \cdots, \beta_L)$ is an $L \times L$ diagonal matrix. The PS model (2) decomposes the channel matrix $\boldsymbol{H}$ in terms of $\boldsymbol{A}_R(\underline{\phi}_R)$, $\boldsymbol{A}_T(\underline{\phi}_T)$, and $\boldsymbol{H}_P$, all of which depend on actual physical parameters. The model is *linear* in the channel gains $\{\beta_l\}$ but *nonlinear* in the spatial angles $\{\phi_{R,l}, \phi_{T,l}\}$.

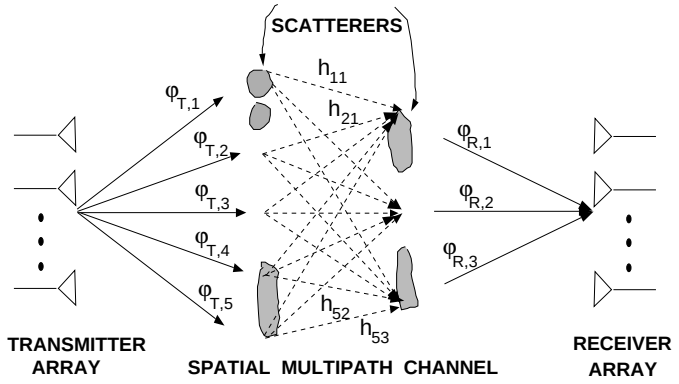


Figure 2: *A schematic illustrating channeling modeling in the* **virtual space**. *The virtual angles are fixed a priori and their spacing is determined by the antenna spacing and defines the spatial resolution — VS channel representation does not distinguish between scatterers that are within the spatial resolution; the scatterers corresponding to the physical angles $\phi_{T,1}$ and $\phi_{T,2}$, for example. The channel is characterized by the coefficients, $\{H_V(p,q) = h_{p,q}\}$, that couple the $n_T$ virtual transmit angles, $\{\varphi_{T,p}\}$, with the $n_R$ virtual receive angles, $\{\varphi_{R,q}\}$. In particular, for angles where there is no significant scattering at the transmitter and/or receiver, the corresponding coefficients are approximately zero (e.g., $h_{21}$ and $h_{52}$).*

The finite dimensionality of the spatial signal space (due to the finite number of antenna elements) can be exploited to develop a *linear* channel model which uses spatial beams in *fixed, virtual* directions at the transmitter and the receiver. The *virtual space*

(VS) model, illustrated in Figure 2, can be expressed as

$$\boldsymbol{H} = \sum_{q=1}^{n_R} \sum_{p=1}^{n_T} H_V(q,p) \boldsymbol{a}_R(\varphi_{R,q}) \boldsymbol{a}_T^H(\varphi_{T,p}) = \widetilde{\boldsymbol{A}}_R \boldsymbol{H}_V \widetilde{\boldsymbol{A}}_T^H \tag{3}$$

where $\{\varphi_{R,q}\}$ and $\{\varphi_{T,p}\}$ are virtual angles that result in full-rank matrices $\widetilde{\boldsymbol{A}}_R = [\boldsymbol{a}_R(\varphi_{R,1}), \cdots, \boldsymbol{a}_R(\varphi_{R,Q})]$ $(n_R \times n_R)$ and $\widetilde{\boldsymbol{A}}_T = [\boldsymbol{a}_T(\varphi_{T,1}), \cdots, \boldsymbol{a}_T(\varphi_{T,P})]$ $(n_T \times n_T)$. The $n_R \times n_T$ matrix $\boldsymbol{H}_V$ is the VS channel representation. The extent of the spatial horizon covered by the virtual angles $\{\varphi_{R,q}\}$ and $\{\varphi_{T,p}\}$ at the receiver and transmitter, respectively, depends on the spacing between the antenna elements. Within the covered spatial horizons, the effect of limited angular *scattering* spreads is captured by the non-zero values of the matrix $\boldsymbol{H}_V$. For smaller angular spreads, only certain sub-matrices of $\boldsymbol{H}_V$ are nonvanishing. In contrast to the PS model (2), the VS model is *linear* and is characterized by the matrix $\boldsymbol{H}_V$ due to the fixed choice of spatial angles. However, in contrast to $\boldsymbol{H}_P$, the matrix $\boldsymbol{H}_V$ is not diagonal in general. Finally, we note that the PS model has $3L$ parameters $\{\beta_l, \phi_{R,l}, \phi_{T,l}\}$, whereas the VS model has $n_T n_R$ parameters (entries of $\boldsymbol{H}_V$).

# 3 The Virtual Space Model

For simplicity of exposition, we develop the VS model in the context of uniform linear arrays (ULAs) at both the transmitter and the receiver with antenna spacings $d_R$ and $d_T$, respectively. Analogous formulations for arbitrary geometries can also be developed. In the case of ULAs, the array steering and response vectors take the form

$$\boldsymbol{a}_T(\phi_T) = \left[1,\ e^{-j2\pi d_T \sin(\phi_T)/\lambda}, \cdots, e^{-j2\pi d_T (n_T-1)\sin(\phi_T)/\lambda}\right]^T \tag{4}$$

$$\boldsymbol{a}_R(\phi_R) = \left[1,\ e^{-j2\pi d_R \sin(\phi_R)/\lambda}, \cdots, e^{-j2\pi d_R (n_R-1)\sin(\phi_R)/\lambda}\right]^T \tag{5}$$

The following represent a natural choice for virtual spatial angles

$$\varphi_{T,p} = \sin^{-1}\left(\frac{p\lambda}{n_T d_T}\right) \quad , \quad \varphi_{R,q} = \sin^{-1}\left(\frac{q\lambda}{n_R d_R}\right) \tag{6}$$

where $p = -(n_T-1)/2, \cdots, (n_T-1)/2$ for $n_T$ odd and $p = -n_T/2, \cdots, n_T/2-1$ for $n_T$ even, and similarly for the index $q$ in (6). For the above choice of angles, the VS matrices $\widetilde{\boldsymbol{A}}_R$ and $\widetilde{\boldsymbol{A}}_T$ are unitary — discrete Fourier transform matrices, in fact. We note that for $d_T = d_R = \lambda/2$, the virtual angles (6) cover the entire ($[-\pi/2, \pi/2]$) spatial horizon. However, larger antenna spacings (covering smaller spatial horizons) may be used in spatial multiplexing applications.

To illustrate the effect of angular scattering spreads on $\boldsymbol{H}_V$, consider a single cluster of contiguous scatters with $S_R = [S_{R-}, S_{R+}] \subset [-\pi/2, \pi/2]$ and $S_T = [S_{T-}, S_{T+}] \subset [-\pi/2, \pi/2]$. In this case, $\boldsymbol{H}_V$ consists of a nonvanishing submatrix corresponding to $S_R$ and $S_T$. In particular, $H_V(p,q)$ are nonzero for $q = Q_-, \cdots, Q_+$, $p = P_-, \cdots, P_+$ where $Q_- \approx \lfloor n_R \sin(S_{R-}) d_R/\lambda \rfloor$, $Q_+ \approx \lceil n_R \sin(S_{R+}) d_R/\lambda \rceil$, and similarly for $P_-$ and $P_+$. For example, for $S_{R-} = -\pi/2$, $S_{R+} = \pi/2$ (maximum spread) and $d_T = d_R = \lambda/2$, $Q_- \approx -n_R/2$ and $Q_+ \approx n_R/2$ (all receive dimensions non-zero). The $\boldsymbol{H}_V$ corresponding to multiple clusters [4] is a superposition of nonvanishing submatrices corresponding to the scattering spreads associated with each cluster.

$\boldsymbol{H}_V$ provides a natural link between PS modeling via $\boldsymbol{H}_P$ and ES modeling via $\boldsymbol{H}$. We can establish this link by relating $\boldsymbol{H}_V$ to the PS matrix $\boldsymbol{H}_P$ and imposing an appropriate statistical model on $\boldsymbol{H}_V$. In particular, we demonstrate that by imposing a progressively more complex structure on $\boldsymbol{H}_V$, we can capture a fairly rich class of ES statistical models with a corresponding physical/propagation interpretation in the PS.

## 3.1 Relationship to Element and Physical Space Models

Since $\widetilde{\boldsymbol{A}}_R$ and $\widetilde{\boldsymbol{A}}_R$ are unitary, $\boldsymbol{H}_V$ is related to $\boldsymbol{H}$ as

$$\boldsymbol{H}_V = \widetilde{\boldsymbol{A}}_R^H \boldsymbol{H} \widetilde{\boldsymbol{A}}_T. \tag{7}$$

This implies that the VS channel representation $\boldsymbol{H}_V$ is *unitarily equivalent* to the ES representation $\boldsymbol{H}$. In fact, the VS matrix $\boldsymbol{H}_V$ can be thought of as a Fourier domain representation of ES channel representation $\boldsymbol{H}$. Thus, $\boldsymbol{H}_V$ captures all channel information and may be used, equivalently, wherever the ES matrix $\boldsymbol{H}$ is used — for example, for capacity calculations and transceiver design. Similarly, $\boldsymbol{H}_V$ is related to $\boldsymbol{H}_P$ as

$$\boldsymbol{H}_V = \widehat{\boldsymbol{A}}_R(\underline{\phi}_R) \boldsymbol{H}_P \widehat{\boldsymbol{A}}_T^H(\underline{\phi}_T) \tag{8}$$

where $\widehat{\boldsymbol{A}}_R(\underline{\phi}_R) = \widetilde{\boldsymbol{A}}_R^H \boldsymbol{A}_R(\underline{\phi}_R) = [\widehat{\boldsymbol{a}}_R(\phi_{R,1}), \cdots, \widehat{\boldsymbol{a}}_R(\phi_{R,L})]$ is a $n_R \times L$ matrix whose columns represent the projection of the PS array response vectors onto the VS array response vectors and $\widehat{\boldsymbol{A}}_T(\underline{\phi}_T) = \widetilde{\boldsymbol{A}}_T^H \boldsymbol{A}_T(\underline{\phi}_T) = [\widehat{\boldsymbol{a}}_T(\phi_{T,1}), \cdots, \widehat{\boldsymbol{a}}_T(\phi_{T,L})]$ is a $n_T \times L$ matrix whose columns represent the projection of the PS steering vectors onto the VS steering vectors. As illustrated in Figure 3, the vector $\widehat{\boldsymbol{a}}_R(\phi_{R,l})$ peaks at the few virtual angles in the neighborhood of the physical angle $\phi_{R,l}$ and a similar interpretation holds for $\widehat{\boldsymbol{a}}_T(\phi_{T,l})$.

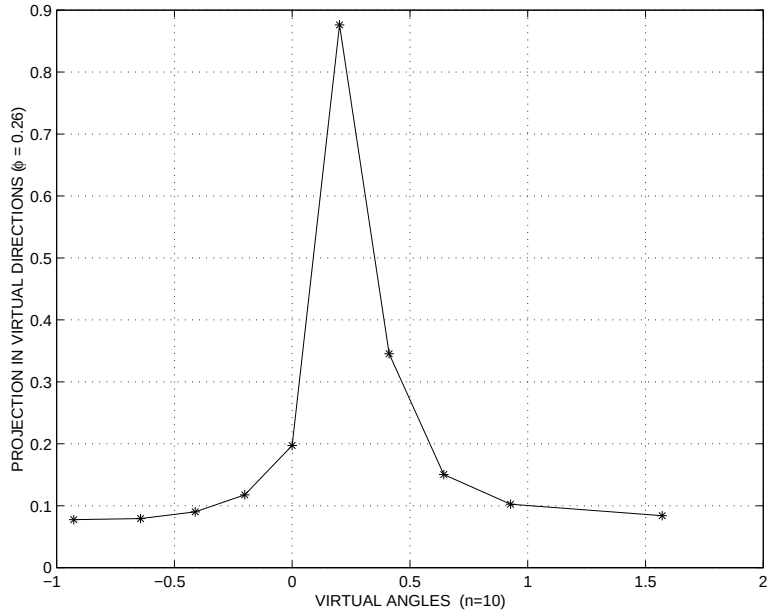


Figure 3: *Magnitude of the projection of a PS array response vector $\boldsymbol{a}(\phi)$ onto the VS array response vectors: $|\widehat{\boldsymbol{a}}(\phi)| = |\widetilde{\boldsymbol{A}}^H \boldsymbol{a}(\phi)|$. In this case, $n = n_T = n_R = 10$. Note that the VS projections peak near the actual physical angle $\phi = 0.26$. Though not illustrated here, the peaks get sharper with larger $n$ (larger signal space dimensions).*

## 3.2 Statistical Channel Modeling in the Virtual Space

In this section, we discuss capturing the statistics of the ES channel matrix $\boldsymbol{H}$ via statistical modeling of $\boldsymbol{H}_V$. From (3) it follows that $\boldsymbol{h} = \mathrm{vec}(\boldsymbol{H}) = [\widetilde{\boldsymbol{A}}_T \otimes \widetilde{\boldsymbol{A}}_R]\boldsymbol{h}_V$, where $\boldsymbol{h}_V = \mathrm{vec}(\boldsymbol{H}_V)$, $\mathrm{vec}(\boldsymbol{H})$ represents a vector obtained by stacking the columns of $\boldsymbol{H}$ and $\otimes$ represents the kronecker product [6]. Here we have used the identity $\mathrm{vec}(\boldsymbol{ADB}) =$

$[\boldsymbol{B}^H \otimes \boldsymbol{A}]\mathrm{vec}(\boldsymbol{D})$ [6]. Let $\boldsymbol{R} = \mathrm{E}[\boldsymbol{h}\boldsymbol{h}^H]$ denote the correlation matrix $\boldsymbol{h}$ and let $\boldsymbol{R}_V$ denote the correlation matrix of $\boldsymbol{h}_V$. The two correlation matrices are related by $\boldsymbol{R} = [\widetilde{\boldsymbol{A}}_T \otimes \widetilde{\boldsymbol{A}}_R]\boldsymbol{R}_V[\widetilde{\boldsymbol{A}}_T^H \otimes \widetilde{\boldsymbol{A}}_R^H]$. $\boldsymbol{R}_V$ is always approximately diagonal[1] but may have some zero diagonal elements due to the sparseness of $\boldsymbol{H}_V$. We note that $\boldsymbol{R}$ and $\boldsymbol{R}_V$ are also unitarily equivalent.

We can obtain a more explicit characterization of $\boldsymbol{h}$ and $\boldsymbol{R}$ from (3)

$$\boldsymbol{h} = \sum_{q=1}^{n_R}\sum_{p=1}^{n_T} H_V(q,p)[\boldsymbol{a}_T(\varphi_{T,p}) \otimes \boldsymbol{a}_R(\varphi_{R,q})] \tag{9}$$

$$\boldsymbol{R} = \sum_{q=1}^{n_R}\sum_{p=1}^{n_T} \sigma_{q,p}^2[\boldsymbol{a}_T(\varphi_{T,p}) \otimes \boldsymbol{a}_R(\varphi_{R,q})][\boldsymbol{a}_T^H(\varphi_{T,p}) \otimes \boldsymbol{a}_R^H(\varphi_{R,q})] \tag{10}$$

where we have assumed that $\{H_V(q,p)\}$ are uncorrelated and $\sigma_{q,p}^2 = \mathrm{E}[|H_V(q,p)|^2]$ is the power in each virtual channel coefficient. From (10) we note that the VS provides an eigen decomposition of $\boldsymbol{R}$, with $\{\boldsymbol{a}_T(\varphi_{T,p}) \otimes \boldsymbol{a}_R(\varphi_{R,q})\}$ serving as the eigenvectors and $\{\sigma_{q,p}^2\}$ the corresponding eigenvalues. (9) is the corresponding Karhunen-Loeve representation.

The relation (10) between $\boldsymbol{R}$ and $\{\sigma_{q,p}^2\}$ provides a systematic way of relating the statistics of the ES model to the actual physical scattering. Suppose that $n_T = n_R = n$ for simplicity of exposition. The $\{\sigma_{q,p}^2\}$ in (10) that are nonzero represent active scattering between the $p^{th}$ transmit element and $q^{th}$ receive virtual element. For simplicity assume that $\sigma_{q,p}^2$ is either 0 or 1. The extreme case of maximally rich scattering corresponds to $\sigma_{q,p}^2 = 1$ for all $p, q$ which results in $\boldsymbol{R} = \boldsymbol{I}$, the iid ES statistical model usually assumed in most capacity calculations. On the other extreme is *diagonally coupled* scattering in which $\sigma_{q,p}^2 = 1$ only if $p = q$ and zero otherwise which results in

$$\boldsymbol{h} = \sum_{p=1}^{n} H_V(p,p)[\boldsymbol{a}_T(\varphi_{T,p}) \otimes \boldsymbol{a}_R(\varphi_{R,p})] \tag{11}$$

$$\boldsymbol{R} = \sum_{p=1}^{n} \sigma_{p,p}^2[\boldsymbol{a}_T(\varphi_{T,p}) \otimes \boldsymbol{a}_R(\varphi_{R,p})][\boldsymbol{a}_T^H(\varphi_{T,p}) \otimes \boldsymbol{a}_R^H(\varphi_{R,p})]. \tag{12}$$

While the VS channel representation is diagonal in this case, there is significant correlation between the various ES channel components of $\boldsymbol{H}$. Intermediate cases between these two extreme cases can be realized by progressively adding minor diagonals to (12) until the relation (10) is attained. This suggests the k-diagonal channel model[2]

$$\boldsymbol{h}_k = \sum_{p=1}^{n} \sum_{q=\max(1,p-k)}^{\min(n,p+k)} H_V(q,p)[\boldsymbol{a}_T(\varphi_{T,p}) \otimes \boldsymbol{a}_R(\varphi_{R,q})] \tag{13}$$

$$\boldsymbol{R}_k = \sum_{p=1}^{n} \sum_{q=\max(1,p-k)}^{\min(n,p+k)} \sigma_{q,p}^2[\boldsymbol{a}_T(\varphi_{T,p}) \otimes \boldsymbol{a}_R(\varphi_{R,q})][\boldsymbol{a}_T^H(\varphi_{T,p}) \otimes \boldsymbol{a}_R^H(\varphi_{R,q})] \tag{14}$$

where $0 \le k \le n-1$. As demonstrated in the next section, this approach for modeling progressively rich scattering in the VS provides a natural link between PS and ES modeling and is very useful in channel capacity calculations. In particular, (10) and (12) have nearly identical ergodic capacities (under appropriate power normalization) but starkly different outage capacities due to higher diversity in (10).

[1] Under the assumption of uncorrelated scattering as a function of spatial angle.

[2] Note that this also represents the orthogonal projection of $\boldsymbol{H}$ onto the space of k-diagonal $\boldsymbol{H}_V$'s since $\widetilde{\boldsymbol{A}}_R$ and $\widetilde{\boldsymbol{A}}_T$ are unitary.

# 4 Capacity Calculations in the Virtual Space

In this section, we discuss channel capacity calculations to illustrate the ease of computation and simple interpretation afforded by the VS model. We first briefly discuss the key parameters that control capacity and relate them to physical propagation characteristics. Our focus here is on outage capacity, a metric more appropriate in fading channels.

## 4.1 Parallel Channels and Diversity

A closer look at (8) reveals that, in essence, $\boldsymbol{H}_V$ provides an "image" of the physical scattering geometry. Recall that $\boldsymbol{H}_P$ is a diagonal matrix. If the physical angles $\{\phi_{R,l}\}$ and $\{\phi_{T,l}\}$ follow similar trends as a function of the path index (monotonically increasing or decreasing), then $\boldsymbol{H}_V$ would also follow a similar diagonal trend with a small spread due to the projection of the physical angles onto the virtual angles. On the other hand, if the coupling between the transmit and receive angles is richer (more cross-coupling between the different transmit and receive virtual angles), it will manifest itself as more nondiagonal terms in $\boldsymbol{H}_V$.

The "image" of the scattering environment provided by $\boldsymbol{H}_V$ is intimately related to two key parameters that affect channel capacity: the number of available *parallel channels*, $P$, that controls ergodic capacity, and the level of *diversity per parallel channel*, $D$, that controls the outage capacity. $P \leq P_{max} = \min(n_T, n_R)$, the rank of $\boldsymbol{H}$, and there have to be at least $L = \min(n_T, n_R)$ distinct paths (resolvable in the virtual space) to achieve $P_{max}$. However, to get maximum diversity, more paths are needed. The maximum diversity per parallel channel is $D_{max} = \max(n_T, n_R)$. In order to achieve $D_{max}$, each virtual angle associated with a parallel channel at the transmitter must be associated with $D_{max}$ different virtual angles via different paths at the receiver. Thus, in order to achieve both $P = P_{max}$ as well as $D = D_{max}$, we need at least $\min(n_T, n_R) \times \max(n_T, n_R) = n_T \times n_R$ distinct paths that are resolvable in the VS. For example, the diagonal model in (12) achieves $P = P_{max}$ but $D = 1$ whereas the full iid model in (10) with all $\sigma^2_{p,q} = 1$ attains $P = P_{max}$ and $D = D_{max}$. We note that the requirement for paths to be resolvable in the VS is important because it is only the paths that correspond to distinct virtual angles that contribute to diversity and parallel channels. In particular, if the paths are confined to an angular spread that is smaller than the spatial resolution (spacing between virtual angles), the corresponding $P$ and $D$ will be close to 1 no matter how large $L$ is.

## 4.2 Capacity Expressions

Now consider the noisy channel, $\boldsymbol{x} = \sqrt{P}\boldsymbol{H}\boldsymbol{s} + \boldsymbol{w}$, where $P$ is the transmitted power ($\mathrm{E}[\|\boldsymbol{s}\|^2] = 1$) and $\boldsymbol{w}$ is zero-mean complex Gaussian noise vector with $\mathrm{E}[\boldsymbol{w}\boldsymbol{w}^H] = \boldsymbol{I}$. In this section, for simplicity of exposition, we fix $n_T = n_R = n$. Given the knowledge of channel coefficients ($\boldsymbol{H}$ or $\boldsymbol{H}_V$) at the receiver, the channel capacity is given by [2, 1]

$$C(\boldsymbol{H}) = \log_2 \left[\det\left(\boldsymbol{I} + P\boldsymbol{H}\boldsymbol{H}^H/n\right)\right] = \log_2 \left[\det\left(\boldsymbol{I} + P\boldsymbol{H}_V\boldsymbol{H}_V^H/n\right)\right] = C(\boldsymbol{H}_V) \ \ bits/s/Hz \tag{15}$$

where the second equality follows from the unitary equivalence of $\boldsymbol{H}$ and $\boldsymbol{H}_V$. The ergodic capacity is given by $C_E = \mathrm{E}[C(\boldsymbol{H}_V)]$ where the expectation is over the statistics of $\boldsymbol{H}_V$. If the propagation environment consists of a cluster of scatterers, the imaging interpretation of $\boldsymbol{H}_V$ implies that it would consist of nonvanishing submatrices corresponding to different clusters. In such cases, the expression (15) can be further simplified to

$$C(\boldsymbol{H}_V) = \sum_{i=1}^{N_c} \log_2 \left[\det(\boldsymbol{I} + P\boldsymbol{H}_V(i)\boldsymbol{H}_V^H(i)/n)\right] \quad bits/s/Hz \tag{16}$$

where $N_c$ is the number of distinct clusters and $\boldsymbol{H}_V(i)$ is the submatrix corresponding to the $i^{th}$ cluster.[3] For example, two $\pi/8$-wide clusters (as seen from either the transmitter or receiver) centered at $\phi_R = \phi_T = \pm\pi/4$ would results in a block diagonal matrix $\boldsymbol{H}_V = \text{diag}(\boldsymbol{H}_V(1), \boldsymbol{H}_V(2))$ with the size of $\boldsymbol{H}_V(i)$'s determined by the number of resolvable virtual angles within the $\pi/8$ angular spreads. Each $\boldsymbol{H}_V(i)$ in (16) can then be represented as a k-diagonal matrix with iid entries representing the nature of scattering within the cluster (the extent of cross-coupling between the transmit and receive virtual angles within the cluster). The cluster decomposition in (16) has the following simple interpretation:

*An arbitrary spatial channel (scattering environment) can be decomposed into $N_c$ independent parallel channels in the VS that are represented by the matrices $\{\boldsymbol{H}_V(i) : i = 1, \cdots, N_c\}$, each $\boldsymbol{H}_V(i)$ in turn representing a k-diagonal iid spatial channel that corresponds to the nature of scattering in each cluster.*

## 4.3 Numerical Examples

We now illustrate capacity computation via $\boldsymbol{H}_V$ for two different environments: An idealized rich scattering environment and a more realistic scattering environment with a smaller scattering angular spread. In all examples, $n_T = n_R = 10$ and SNR $= 10\log_{10}(P)$ $= 20$dB.

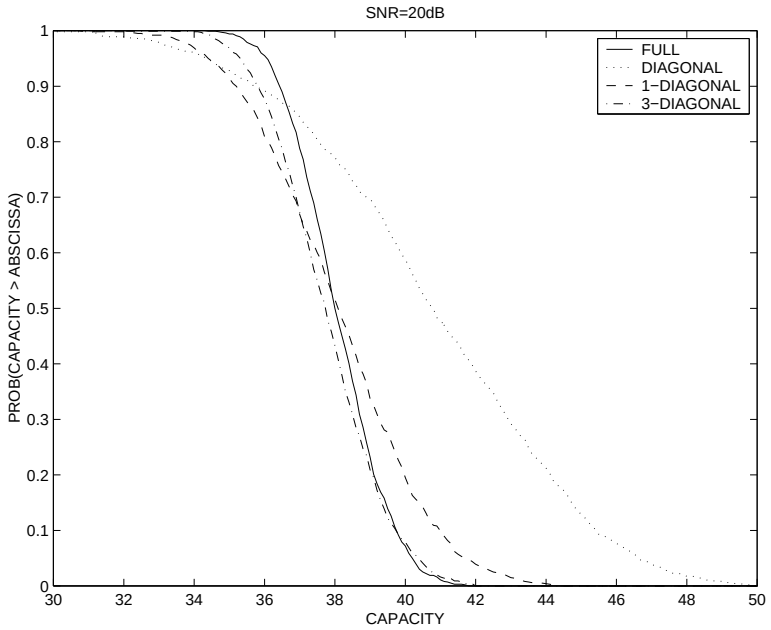


Figure 4: *Capacity comparison in a rich scattering environment with energy normalization so that all models have the same received SNR. The level of diversity, D, is the main difference between various models.*

Consider the rich scattering case. The channel in this case is directly modeled via (1) with the elements of $\boldsymbol{H}$ given by iid complex zero-mean Gaussian random variables with unit variance. We compare the capacity of a full iid model with a k-diagonal VS system. Two separate comparisons are made. In the first comparison, illustrated in Figure 4, the k-diagonal VS matrix is scaled so that the received SNR is the same as in the full iid case. The scaling factor is given by $n^2/(n + k(2n - k - 1))$, $k = 0, \cdots, n - 1$, which

[3]The relation (16) assumes that each cluster corresponds to distinct transmit and receive virtual angles. However, this assumption can be relaxed and a relation of the form (16) can be derived in that case as well.

equals $n$ for $k = 0$ (diagonal approximation) and 1 for $k = (n-1)$ (full matrix). This comparison captures the effect of diversity on outage capacity — a $k$ diagonal system provides higher values of $D$ with increasing $k$. As evident from Figure 4, the performance of a 3-diagonal system is very close to the full system ($k = 9$), demonstrating that for the same received SNR the 3-diagonal system captures most of the diversity advantage. We note that the ergodic capacity of the all systems is virtually identical in this case. The second comparison, illustrated in Figure 5, does not normalize the received energy can be thought of as a comparison of the full iid channel with that of a k-diagonal VS approximation (projection of the full channel onto the space of k-diagonal channels). Both the received SNR and diversity are at play in this case. As evident from Figure 5, the diagonal approximation is very poor but the 5-diagonal approximation comes within 5% of the capacity of the full iid system. This suggests that even in an idealized rich scattering environment, k-diagonal VS approximations with moderate values of k can be quite adequate. Note that k-diagonal systems result in simpler transceiver structures due to fewer channel parameters.

Figure 6 compares the capacity of a channel with k-diagonal VS approximations in the VS under a more realistic scattering environment with no SNR normalization. In this case, the channel matrix $\boldsymbol{H}$ is simulated via the physical model (2) corresponding to two $\pi/8$-wide clusters (as seen from either the transmitter or receiver) centered at $\phi_R = \phi_T = \pm\pi/4$. There are $L = 50$ paths in each cluster. The angles $\{\phi_{T,l}, \phi_{R,l}\}$ for the paths are uniformly distributed over the angular spreads and the corresponding fading gains $\{\beta_l\}$ are simulated as iid zero mean complex Gaussian random variables with unit variance. As evident from Figure 6, the capacity of a 2-diagonal system is very close to that of the full (9-diagonal) system. This is due to the fact that $D$ is relatively small in this case due to limited angular scattering spread and is adequately captured by a 2-diagonal system (significant correlation between the elements of $\boldsymbol{H}$).

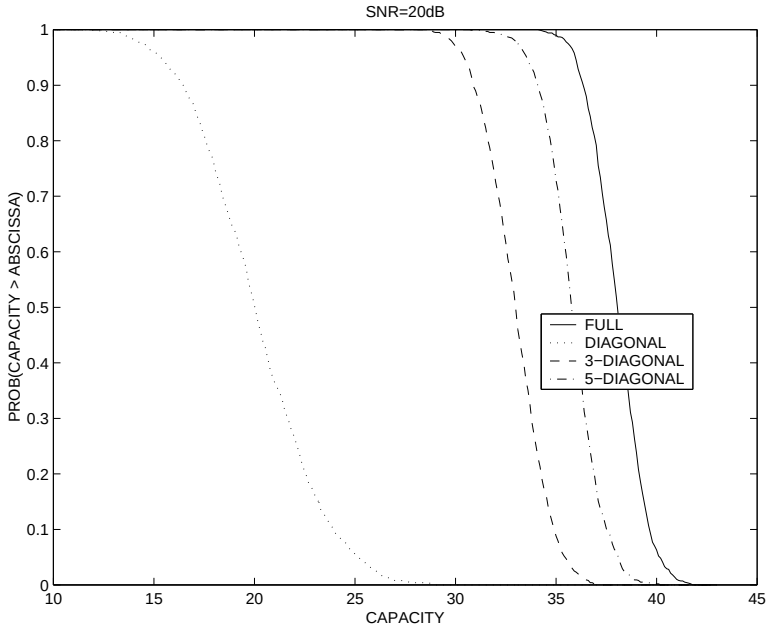


Figure 5: *Capacity comparison without energy normalization in a rich scattering environment. Both received SNR and diversity affect capacity in this case.*

# 5 Conclusions

We have proposed a virtual space (VS) framework for modeling multi-antenna multipath channels that provides a natural link between various existing modeling approaches. In

particular, it captures physical propagation effects in a linear fashion via the notion of virtual spatial angles and provides a direct handle on computing the corresponding channel statistics. The VS channel model facilitates accurate estimates of channel capacity in realistic scattering environments. It clearly reveals the two key parameters affecting capacity: the number of parallel channels and the level of diversity per parallel channel. While the focus of this paper is on spatial effects, the framework can be readily extended to include the temporal dimension and such extensions will be reported elsewhere. Finally, the framework suggests direct extensions for modeling spatial multiplexing schemes.[4]

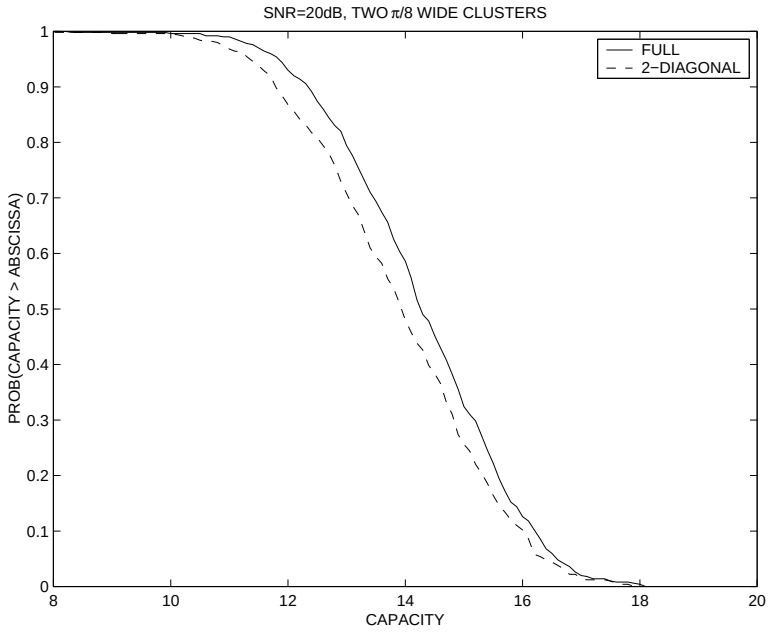


Figure 6: *Capacity comparison without energy normalization in a realistic scattering environment consisting of two $\pi/8$-wide clusters.*

# References


[1] E. Telatar, "Capacity of multi-antenna gaussian channels," *AT& T-Bell Labs Internal Tech. Memo.*, June 1995.

[2] G. J. Foschini, "Layered space-time architecture for wireless communication in a fading environment when using multi-element antennas," *Bell Labs Tech. J.*, vol. 1, no. 2, pp. 41–59, 1996.

[3] V. Tarokh, N. Seshadri, and A. R. Calderbank, "Space-time codes for high data rate wireless communication: Performance criteria and code construction," *IEEE Trans. Inform. Th.*, pp. 744–765, Mar. 1998.

[4] J. Fuhl, A. F. Molisch, and E. Bonek, "Unified channel model for mobile radio systems with smart antennas," in *IEE Proc. Radar, Sonar Navig.*, vol. 145, pp. 32–41, Feb. 1998.

[5] G. G. Raleigh and J. M. Cioffi, "Spatio-temporal coding for wireless communication," *IEEE Trans. Commun.*, pp. 357–366, Mar. 1998.

[6] J. W. Brewer, "Kronecker products and matrix calculus in system theory," *IEEE Trans. Circ. and Syst.*, vol. 25, pp. 772–781, Sep. 1978.


[4] R. W. Heath, Jr. Personal communication.